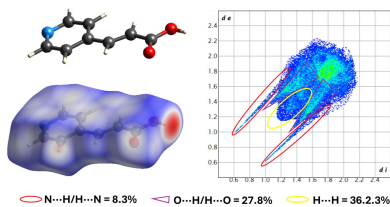# research communications

Synthesis, characterization and supramolecular analysis for (E)-3-(pyridin-4-yl)acrylic acid

Valentina Florez-Muñoz,[a] Andres Felipe Guerrero,[a] Mario Macias,[b] Luis Alberto Illicachi[a]* and Richard D'Vries[c]*

[a]Facultad de Ciencias Básicas, Universidad Santiago de Cali, Calle 5 No 62-00, Cali, Colombia, [b]Cristalografía y Química de Materiales (CrisQuimMat), Facultad de Ciencias, Departamento de Química, Universidad de los Andes, Cra. 1 No 18a-12, Bogotá, Colombia, and [c]Facultad de Ciencias Naturales, Exactas y de la Educación, Departamento de Química, Universidad del Cauca, Calle 5 No 4-70, Popayán, Colombia. *Correspondence e-mail: luis.illicachi00@usc.edu.co, richard.dvries@unicauca.edu.co
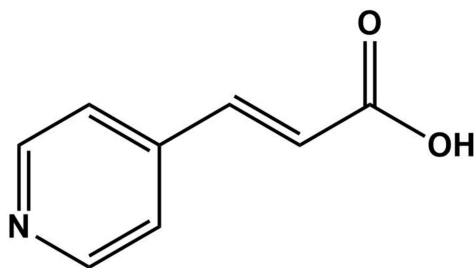
The title compound, $C_8H_7NO_2$, crystallizes as prismatic colourless crystals in space group $P\bar{1}$, with one molecule in the asymmetric unit. The pyridine ring is fused to acrylic acid, forming an almost planar structure with an E-configuration about the double bond with a torsion angle of $-6.1\,(2)°$. In the crystal, strong O—H···N interactions link the molecules, forming chains along the [101] direction. Weak C—H···O interactions link adjacent chains along the [100] direction, generating an $R_2^2(14)$ homosynthon. Finally, π–π stacking interactions lead to the formation of the three-dimensional structure. The supramolecular analysis was supported by Hirshfeld surface and two-dimensional fingerprint plot analysis, indicating that the most abundant contacts are associated with H···H, O···H/H···O, N···H/H···N and C···H/H···C interactions.

1. Chemical context

Cinnamic acid and its derivatives have been used in several applications related to medicinal chemistry (Deng *et al.*, 2023), organic synthesis (Chen *et al.*, 2020), and coordination chemistry (Zhou *et al.*, 2016). Cinnamic acids are reactive molecules due to possessing an unsaturated carbonyl moiety, which can be considered a Michael acceptor and benzene ring. Both make it possible to modify them, resulting in synthetic cinnamic acid derivatives with a broad range of biological properties, including antibacterial (Ruwizhi & Aderibigbe, 2020) antituberculosis (Teixeira *et al.*, 2020), antimalarial (Fonte *et al.*, 2023), antidiabetic (Adisakwattana, 2017; Feng *et al.*, 2022), anticancer (Feng *et al.*, 2022), antifungal (Liu *et al.*, 2024), Alzheimer's treatment (Drakontaeidi & Pontiki, 2024), antioxidant (Nouni *et al.*, 2023), and cosmetic (Gunia-Krzyżak *et al.*, 2018). Among the various types of cinnamic acids documented, 4-pyridylacrylic acid (4-Hpya) is considered a highly valuable ligand because of several structural characteristics that make it suitable for the construction of coordination compounds. These characteristics include multiple coordination sites, which enable the formation of higher-dimensional structures, and versatile coordination modes to form different structures (Khalfaoui *et al.*, 2021). On the other hand, its capacity to function as both a hydrogen-bond donor and acceptor facilitates the creation of intricate hydrogen-bonded networks (Jiao *et al.*, 2007; Zhu *et al.*, 2005).

N···H/H···N = 8.3% O···H/H···O = 27.8% H···H = 36.2.3%

Table 1
Hydrogen-bond geometry (Å, °).

$D—H\cdots A$	$D—H$	$H\cdots A$	$D\cdots A$	$D—H\cdots A$
O1—H1$\cdots$N1[i]	0.99 (3)	1.63 (3)	2.6147 (18)	177 (3)
C5—H5$\cdots$O2[ii]	0.93	2.57	3.336 (2)	140

Symmetry codes: (i) $x + 1, y, z - 1$; (ii) $-x + 1, -y + 2, -z + 2$.

2. Structural commentary

The title compound crystallizes in space group $P\bar{1}$ with one molecule per asymmetric unit (Fig. 1). The pyridinic ring is fused to acrylic acid, forming an almost planar structure with an *E*-configuration about the double bond, with a C8—C4—C3—C2 torsion angle of −6.1 (2)°.

3. Supramolecular features

In the crystal, strong O1—H1$\cdots$N1 interactions link the molecules, forming chains along the [101] direction (Fig. 2*a*, Table 1). Adjacent chains are linked along the [100] direction through weak C—H$\cdots$O interactions, generating an $R_2^2(14)$ homosynthon (Fig. 2*b*). Finally, the three-dimensional supramolecular structure is finally formed by slipped π–π stacking interactions (Hunter & Sanders, 1990) between the pyridinic rings (N1/C4–C8) with distances of 3.8246 (10) Å, and π–π stacking interactions of the acrylic double bond (C2=C3) of 3.4322 (10)Å (Fig. 2*c*). An interaction between the nitrogen atom of the pyridinic ring, N1, and the double bond of the acrylic group with a distance of 3.4044 (13) Å is also observed.

A Hirshfeld surface analysis was performed to confirm, visualise and quantify the supramolecular interactions present in title compound. The Hirshfeld surface mapped over d_{norm} and 2D fingerprint plots (Spackman & Jayatilaka, 2009) were generated using *Crystal Explorer 17* (Spackman, *et al.*, 2021). Fig. 3 shows the strongest interactions as red spots. These are associated with the donor and acceptor atoms, in this case for the O—H$\cdots$N interaction. The weakest interactions, associated with the C—H$\cdots$O contacts, are shown as white areas.
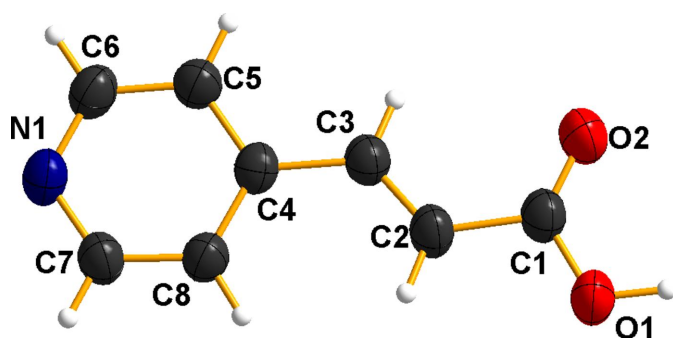
These interactions were quantified through the fingerprint plots, indicating that the most abundant contacts are associated with H$\cdots$H interactions (36.2%) while O$\cdots$H/H$\cdots$O, N$\cdots$H/H$\cdots$N and C$\cdots$H/H$\cdots$C interactions represent 27.8%, 8.7% and 10.7%, respectively. These results show that crystal packing is governed mainly by dispersion and electrostatic interactions.

4. Database survey

A search of the Cambridge Structural Database (Version 2023.3.0; Groom *et al.*, 2016) using Conquest (Bruno *et al.*, 2002) found seven entries for (*E*)-3-(pyridin-4-yl)acrylic acid derivative molecules. In all cases, the protonation of the nitrogen atom in the pyridine ring leads to the formation of pyridinium salts. These include halides (Hu, 2010; Kole *et al.*, 2010), trifluoroacetate (Kole *et al.*, 2010), hydrogen sulfate (Kole *et al.*, 2010), perchlorate and hexafluorophosphate (Kole *et al.*, 2011).

Figure 2
Supramolecular interactions in the title compound. (*a*) O—H$\cdots$N interactions forming chains, (*b*) two chains joined by C—H$\cdots$O interactions and (*c*) π–π stacking interactions between the pyridine rings and the acrylic group.

Figure 1
The molecule of (*E*)-3-(pyridin-4-yl)acrylic acid compound with displacement ellipsoids drawn at the 50% probability level.

N$\cdots$H/H$\cdots$N = 8.3%   O$\cdots$H/H$\cdots$O = 27.8%   H$\cdots$H = 36.2.3%

Figure 3
Hirshfeld surface and fingerprint plot analysis for the title compound.

Figure 4
Reaction scheme for obtaining (*E*)-3-(pyridin-4-yl)acrylic acid.
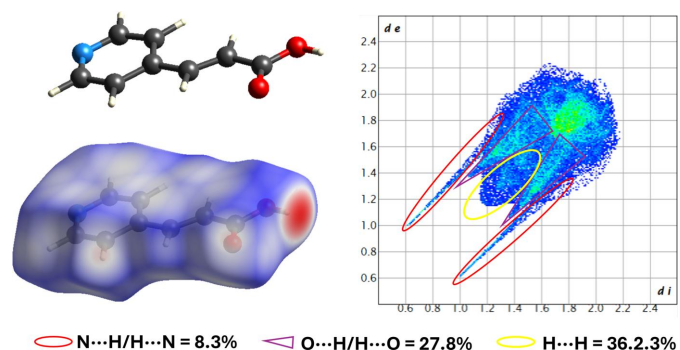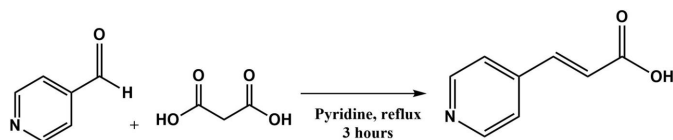
5. Synthesis and crystallization

The synthesis of (*E*)-3-(pyridin-4-yl)acrylic acid compound was performed following the procedure reported by Kudelko *et al.* (2015) for the synthesis of 3-(pyridyl)acrylic acids (Fig. 4). In a 25 mL flat-bottomed flask, 728 mg of malonic acid (0.335 mmol) and 300 mg of 4-pyridincarboxyaldehyde (0.335 mmol) were mixed with 2 ml of pyridine. The reaction mixture was refluxed under constant stirring for 3 h. The reaction synthesis was ice-cooled, and then drops of 37% HCl were added until precipitate formation was observed. The obtained solid was separated by filtration and washed with acetone. The solid product was recrystallized by slow water evaporation, giving a colourless crystalline powder and small prismatic crystals in 97.9% yield.

6. Refinement

Crystal data, data collection and structure refinement details are summarized in Table 2. The O-bound hydrogen atom (H1) was found in electron density maps and freely refined. C-bound hydrogen atoms were positioned geometrically and refined using a riding model [C—H = 0.93 Å, $U_{iso}(H)$ = $1.2U_{eq}(C)$].

Table 2
Experimental details.

Crystal data	
Chemical formula	$C_8H_7NO_2$
M_r	149.15
Crystal system, space group	Triclinic, $P\bar{1}$
Temperature (K)	291
a, b, c (Å)	6.6279 (15), 7.3272 (12), 8.2308 (15)
α, β, γ (°)	67.271 (17), 83.403 (17), 73.006 (17)
V (Å^3)	352.57 (13)
Z	2
Radiation type	Cu $K\alpha$
μ (mm^{-1})	0.85
Crystal size (mm)	$0.09 \times 0.06 \times 0.05$
Data collection	
Diffractometer	SuperNova, Dual, Cu at home/near, Atlas
Absorption correction	Multi-scan (*CrysAlis PRO*; Rigaku OD, 2021)
T_{min}, T_{max}	0.831, 1.000
No. of measured, independent and observed [$I > 2\sigma(I)$] reflections	3635, 1461, 1243
R_{int}	0.035
$(\sin \theta/\lambda)_{max}$ (Å^{-1})	0.631
Refinement	
$R[F^2 > 2\sigma(F^2)], wR(F^2), S$	0.049, 0.153, 1.04
No. of reflections	1461
No. of parameters	104
H-atom treatment	H atoms treated by a mixture of independent and constrained refinement
$\Delta\rho_{max}, \Delta\rho_{min}$ (e Å^{-3})	0.14, −0.27

Computer programs: *CrysAlis PRO* (Rigaku OD, 2021), *SHELXT* (Sheldrick, 2015a), *SHELXL2016/6* (Sheldrick, 2015b) and *OLEX2* (Dolomanov *et al.*, 2009).

References

Adisakwattana, S. (2017). *Nutrients*, **9**, 163.
Bruno, I. J., Cole, J. C., Edgington, P. R., Kessler, M., Macrae, C. F., McCabe, P., Pearson, J. & Taylor, R. (2002). *Acta Cryst.* B**58**, 389–397.
Chen, L., Zhang, L., Yan, G. & Huang, D. (2020). *Asia. J. Org. Chem.* **9**, 842–862.
Deng, H., Xu, Q., Guo, H.-Y., Huang, X., Chen, F., Jin, L., Quan, Z.-S. & Shen, Q.-K. (2023). *Phytochemistry*, **206**, 113532.
Dolomanov, O. V., Bourhis, L. J., Gildea, R. J., Howard, J. A. K. & Puschmann, H. (2009). *J. Appl. Cryst.* **42**, 339–341.
Drakontaeidi, A. & Pontiki, E. (2024). *Int. J. Mol. Sci.* **25**, 582.
Feng, L.-S., Cheng, J.-B., Su, W.-Q., Li, H.-Z., Xiao, T., Chen, D.-A. & Zhang, Z.-L. (2022). *Arch. Pharm.* **355**, 2200052.
Fonte, M., Fontinha, D., Moita, D., Caño-Prades, O., Avalos-Padilla, Y., Fernàndez-Busquets, X., Prudêncio, M., Gomes, P. & Teixeira, C. (2023). *Eur. J. Med. Chem.* **258**, 115575.
Groom, C. R., Bruno, I. J., Lightfoot, M. P. & Ward, S. C. (2016). *Acta Cryst.* B**72**, 171–179.
Gunia–Krzyżak, A., Słoczyńska, K., Popiół, J., Koczurkiewicz, P., Marona, H. & Pękala, E. (2018). *Int. J. Cosmet. Sci.* **40**, 356–366.
Hunter, C. A. & Sanders, J. K. M. (1990). *J. Am. Chem. Soc.* **112**, 5535–5534.
Hu, D.-Y. (2010). *Acta Cryst.* E**66**, o1639.
Jiao, C. M., Zhang, W. H., Tang, X. Y., Liu, L. L., Zhang, Y. & Lang, J. P. (2007). *Inorg. Chem. Commun.* **10**, 975–978.
Khalfaoui, O., Beghidja, A., Beghidja, C., Guari, Y., Larionova, J. & Long, J. (2021). *Polyhedron*, **207**, 115366.
Kole, G. K., Tan, G. K. & Vittal, J. J. (2010). *Org. Lett.* **12**, 128–131.
Kole, G. K., Tan, G. K. & Vittal, J. J. (2011). *Org. Lett.* **76**(19), 7860–7865.
Kudelko, A., Jasiak, K. & Ejsmont, K. (2015). *Monatsh. Chem.* **146**, 303–311.
Liu, H., Cai, C., Zhang, X., Li, W., Ma, Z., Feng, J., Liu, X. & Lei, P. (2024). *J. Agric. Food Chem.* **72**, 2492–2500.
Nouni, C., Theodosis-Nobelos, P. & Rekka, E. A. (2023). *Molecules*, **28**, 6732.
Rigaku OD (2021). *CrysAlis PRO*. Rigaku Oxford Diffraction, Yarnton, England.
Ruwizhi, N. & Aderibigbe, B. A. (2020). *Int. J. Mol. Sci.* **21**, 5712.
Sheldrick, G. M. (2015a). *Acta Cryst.* A**71**, 3–8.
Sheldrick, G. M. (2015b). *Acta Cryst.* C**71**, 3–8.
Spackman, M. A. & Jayatilaka, D. (2009). *CrystEngComm*, **11**, 19–32.

Spackman, P. R., Turner, M. J., McKinnon, J. J., Wolff, S. K., Grimwood, D. J., Jayatilaka, D. & Spackman, M. A. (2021). *J. Appl. Cryst.* **54**, 1006–1011.

Teixeira, C., Ventura, C., Gomes, J. R. B., Gomes, P. & Martins, F. (2020). *Molecules*, **25**, 456.

Zhou, K., Feng, Z., Shen, J., Wu, B., Luo, X., Jiang, S., Li, L. & Zhou, X. (2016). *Spectrochim. Acta A Mol. Biomol. Spectrosc.* **158**, 29–33.

Zhu, Y. J., Chen, J. X., Zhang, W. H., Ren, Z. G., Zhang, Y., Lang, J. P. & Ng, S. W. (2005). *J. Organomet. Chem.* **690**, 3479–3487.

Synthesis, characterization and supramolecular analysis for (*E*)-3-(pyridin-4-yl)acrylic acid

Valentina Florez-Muñoz, Andres Felipe Guerrero, Mario Macias, Luis Alberto Illicachi and Richard D'Vries

Computing details

(*E*)-3-(Pyridin-4-yl)prop-2-enoic acid

Crystal data

$C_8H_7NO_2$	$F(000) = 156$
$M_r = 149.15$	$D_x = 1.405$ Mg m^{-3}
Triclinic, $P\bar{1}$	Melting point: 553 K
$a = 6.6279$ (15) Å	Cu $K\alpha$ radiation, $\lambda = 1.54184$ Å
$b = 7.3272$ (12) Å	Cell parameters from 1657 reflections
$c = 8.2308$ (15) Å	$\theta = 6.8$–74.9°
$\alpha = 67.271$ (17)°	$\mu = 0.85$ mm^{-1}
$\beta = 83.403$ (17)°	$T = 291$ K
$\gamma = 73.006$ (17)°	Prismatic, colourless
$V = 352.57$ (13) Å^3	$0.09 \times 0.06 \times 0.05$ mm
$Z = 2$	

Data collection

SuperNova, Dual, Cu at home/near, Atlas diffractometer	$T_{min} = 0.831$, $T_{max} = 1.000$
Radiation source: micro-focus sealed X-ray tube, SuperNova (Cu) X-ray Source	3635 measured reflections
	1461 independent reflections
Mirror monochromator	1243 reflections with $I > 2\sigma(I)$
Detector resolution: 10.6144 pixels mm^{-1}	$R_{int} = 0.035$
ω scans	$\theta_{max} = 76.6°$, $\theta_{min} = 5.8°$
Absorption correction: multi-scan (CrysAlisPro; Rigaku OD, 2021)	$h = -8 \rightarrow 7$
	$k = -8 \rightarrow 9$
	$l = -10 \rightarrow 10$

Refinement

Refinement on F^2	Hydrogen site location: mixed
Least-squares matrix: full	H atoms treated by a mixture of independent and constrained refinement
$R[F^2 > 2\sigma(F^2)] = 0.049$	
$wR(F^2) = 0.153$	$w = 1/[\sigma^2(F_o^2) + (0.0977P)^2 + 0.0215P]$ where $P = (F_o^2 + 2F_c^2)/3$
$S = 1.04$	
1461 reflections	$(\Delta/\sigma)_{max} < 0.001$
104 parameters	$\Delta\rho_{max} = 0.14$ e Å^{-3}
0 restraints	$\Delta\rho_{min} = -0.27$ e Å^{-3}

Special details

Geometry. All esds (except the esd in the dihedral angle between two l.s. planes) are estimated using the full covariance matrix. The cell esds are taken into account individually in the estimation of esds in distances, angles and torsion angles; correlations between esds in cell parameters are only used when they are defined by crystal symmetry. An approximate (isotropic) treatment of cell esds is used for estimating esds involving l.s. planes.

Fractional atomic coordinates and isotropic or equivalent isotropic displacement parameters (Å²)

	x	*y*	*z*	U_{iso}*/U_{eq}
O1	0.48195 (18)	0.6974 (2)	0.64537 (15)	0.0609 (4)
O2	0.63738 (19)	0.8136 (2)	0.79722 (16)	0.0669 (4)
C2	0.3116 (2)	0.7317 (2)	0.89960 (18)	0.0484 (4)
H2	0.211812	0.676180	0.879516	0.058*
N1	−0.20475 (19)	0.72846 (17)	1.42131 (15)	0.0504 (4)
C5	0.1186 (2)	0.8159 (2)	1.31387 (18)	0.0490 (4)
H5	0.228403	0.862808	1.329376	0.059*
C4	0.1149 (2)	0.76641 (18)	1.16689 (16)	0.0426 (3)
C7	−0.2089 (2)	0.6805 (2)	1.28079 (19)	0.0507 (4)
H7	−0.320055	0.632669	1.269716	0.061*
C1	0.4937 (2)	0.75386 (19)	0.77647 (17)	0.0477 (4)
C3	0.2868 (2)	0.7884 (2)	1.03649 (18)	0.0456 (3)
H3	0.386535	0.847081	1.051782	0.055*
C8	−0.0552 (2)	0.6991 (2)	1.15114 (18)	0.0483 (4)
H8	−0.065343	0.666782	1.054192	0.058*
C6	−0.0433 (3)	0.7943 (2)	1.43650 (18)	0.0524 (4)
H6	−0.038863	0.827444	1.534078	0.063*
H1	0.600 (4)	0.713 (4)	0.561 (3)	0.099 (8)*

Atomic displacement parameters (Å²)

	U^{11}	U^{22}	U^{33}	U^{12}	U^{13}	U^{23}
O1	0.0601 (7)	0.0851 (8)	0.0546 (6)	−0.0366 (6)	0.0209 (5)	−0.0374 (5)
O2	0.0631 (7)	0.0930 (9)	0.0644 (7)	−0.0440 (6)	0.0193 (5)	−0.0389 (6)
C2	0.0493 (8)	0.0521 (7)	0.0490 (8)	−0.0225 (6)	0.0125 (6)	−0.0213 (6)
N1	0.0545 (7)	0.0513 (6)	0.0463 (6)	−0.0184 (5)	0.0129 (5)	−0.0197 (5)
C5	0.0523 (8)	0.0528 (7)	0.0489 (7)	−0.0218 (6)	0.0056 (6)	−0.0225 (6)
C4	0.0457 (7)	0.0396 (6)	0.0405 (7)	−0.0122 (5)	0.0055 (5)	−0.0139 (5)
C7	0.0482 (7)	0.0572 (7)	0.0524 (7)	−0.0224 (6)	0.0101 (6)	−0.0233 (6)
C1	0.0508 (7)	0.0488 (7)	0.0451 (7)	−0.0201 (5)	0.0097 (5)	−0.0167 (5)
C3	0.0455 (7)	0.0468 (6)	0.0450 (7)	−0.0168 (5)	0.0058 (5)	−0.0161 (5)
C8	0.0513 (7)	0.0552 (7)	0.0453 (7)	−0.0202 (6)	0.0075 (5)	−0.0240 (5)
C6	0.0621 (9)	0.0553 (7)	0.0458 (7)	−0.0199 (6)	0.0091 (6)	−0.0249 (6)

Geometric parameters (Å, º)

O1—C1	1.3135 (17)	C5—C4	1.3954 (18)
O1—H1	0.98 (3)	C5—C6	1.386 (2)
O2—C1	1.2110 (19)	C4—C3	1.4729 (19)

C2—H2	0.9300	C4—C8	1.392 (2)
C2—C1	1.4887 (18)	C7—H7	0.9300
C2—C3	1.322 (2)	C7—C8	1.384 (2)
N1—C7	1.3374 (18)	C3—H3	0.9300
N1—C6	1.332 (2)	C8—H8	0.9300
C5—H5	0.9300	C6—H6	0.9300
C1—O1—H1	113.5 (14)	C8—C7—H7	118.6
C1—C2—H2	118.9	O1—C1—C2	112.14 (13)
C3—C2—H2	118.9	O2—C1—O1	124.20 (13)
C3—C2—C1	122.27 (14)	O2—C1—C2	123.65 (13)
C6—N1—C7	117.87 (12)	C2—C3—C4	125.60 (14)
C4—C5—H5	120.4	C2—C3—H3	117.2
C6—C5—H5	120.4	C4—C3—H3	117.2
C6—C5—C4	119.18 (13)	C4—C8—H8	120.2
C5—C4—C3	119.41 (13)	C7—C8—C4	119.52 (12)
C8—C4—C5	117.36 (12)	C7—C8—H8	120.2
C8—C4—C3	123.22 (12)	N1—C6—C5	123.17 (12)
N1—C7—H7	118.6	N1—C6—H6	118.4
N1—C7—C8	122.88 (14)	C5—C6—H6	118.4
N1—C7—C8—C4	1.3 (2)	C3—C2—C1—O2	4.3 (2)
C5—C4—C3—C2	174.27 (12)	C3—C4—C8—C7	179.26 (12)
C5—C4—C8—C7	−1.2 (2)	C8—C4—C3—C2	−6.1 (2)
C4—C5—C6—N1	−0.2 (2)	C6—N1—C7—C8	−0.8 (2)
C7—N1—C6—C5	0.3 (2)	C6—C5—C4—C3	−179.79 (12)
C1—C2—C3—C4	−178.21 (11)	C6—C5—C4—C8	0.6 (2)
C3—C2—C1—O1	−176.96 (13)		

Hydrogen-bond geometry (Å, º)

D—H⋯A	D—H	H⋯A	D⋯A	D—H⋯A
O1—H1⋯N1[i]	0.99 (3)	1.63 (3)	2.6147 (18)	177 (3)
C5—H5⋯O2[ii]	0.93	2.57	3.336 (2)	140

Symmetry codes: (i) $x+1, y, z−1$; (ii) $−x+1, −y+2, −z+2$.

Hydrogen bonds and interactions geometry, (Å, °)

D—H⋯A	D—H	H⋯A	D⋯A	D—H⋯A
O1—H1⋯N1i	0.990 (3)	1.630 (3)	2.61470 (18)	177.0 (3)
C5—H5⋯O2ii	0.9300	2.5700	3.3360 (2)	140.00
Cp1⋯Cp1			3.82460 (10)	
Cp2⋯Cp2			3.43220 (10)	
N1⋯Cp1			3.40440 (13)	